On implementation of feedback-based PD-type iterative learning control for robotic manipulators with hard input constraints

Gijo Sebastian, Zeyu Li, Ying Tan, Denny Oetomo

***Abstract*— It is well-known that a robotic manipulator with the position output has a relative degree 2. A standard feed-forward iterative learning control (ILC) requires the second derivative of the tracking error to achieve a perfect tracking performance. This leads to implementation issues when the output signals are noisy. To address such an issue, this paper presents a feedback-based PD-type ILC with the consideration of the actuator saturation, in which only the first derivative of the tracking error is needed. With the help of a composite energy function, under mild assumptions, Theorem 1 shows that the proposed feedback-based PD-type ILC can ensure perfect tracking performance in the presence of actuator saturation. The simulation and experimental results show the effectiveness of the proposed method.**

I. INTRODUCTION

Driven from many engineering applications, the idea of using past tracking performance in a repetitive tracking task to "learn" the desired control input was proposed by [1] and [2]. Due to its ability to learn over repetitions, this method can relax the requirement of the knowledge of the engineered systems. Hence, this so-called iterative learning control (ILC) algorithm, which is a model-free method, is attractive in various applications such as chemical batch processes [3], energy generation [4], industrial robots [5] and freeway traffic control [6], More details on the various developments and wide applications can be found in the survey papers [7], [8] and references there in.

Many ILC algorithms have been successfully applied to robotic manipulators [2], [9]–[11]. As the relative degree of robotic manipulators with position output is 2, a DD-type ILC which uses the second derivative of tracking error can ensure a perfect tracking performance if a convergence condition is satisfied [12]. When implementing such a DD-type ILC, if the position signals have measurement noises, computing the second derivative of the tracking error without magnifying the high-frequency noises is very challenging. Appropriate filters are needed to filter out high frequency noises without sacrificing the tracking performance. If the filters are not designed appropriately, the tracking error might diverge in the iteration domain.

In order to simplify the implementation of ILC algorithms, instead of using DD-type ILC, a PD-type ILC is used in this paper. That is, the *first* derivative of the tracking error as well as the tracking error are used in the ILC updating laws. This idea was motivated from the works of [13], [14]. The work presented in [13] was focused on the linearized model of robot manipulators, later extended to nonlinear dynamics in [14].

Other than the PD-type feed-forward ILC scheme proposed, a PD-feedback is always used in combination with the feed-forward ILC to enhance the robustness, or ensure the satisfaction of output constraints or improve the transient response in iteration domain.

In robotic manipulators, the motors have limited actuation capabilities. This work extends the results of [14] with the consideration of actuator saturation. The existence of the actuator saturation makes it difficult to have a high gain feed-back controller. Such actuator limitations will have great impact in the implementation of feedback-based PD-type ILC algorithm, leading to a possible divergent performance.

This paper proposes a feedback-based PD-type ILC algorithm that is able to handle input constraints from actuators for robotic manipulators with the relative degree 2. To the best of authors' knowledge, actuator saturation has not been addressed for a feedback-based PD-type ILC algorithm for robotic manipulators in ILC literature, though feed-forward ILC schemes can handle input saturation [15].

This paper extends our previous works on input constraints, [16] and [17], with the consideration of implementation issues. More precisely, instead of using DD-type ILC, this work proposed PD-type ILC in combination of feedback controller to ensure the perfect tracking performance in the presence of hard input constraints (or actuator constraints). As can be seen clearly from experimental results, the feedback-based DD-type ILC cannot work, though simulation results work. The modifications from DD-type ILC to PD-type ILC makes it easy to implement the desired controller as shown in the experimental results.

II. PRELIMINARIES AND PROBLEM FORMULATION

Firstly, the notations used in this paper are introduced, followed by definitions and lemmas. The set of real number and natural numbers are denoted by $\mathcal{R}$ and $\mathcal{N}$ respectively. The set of all continuous functions in a finite time interval, $[0,\ T_f]$ that is differentiable up to j^{th} order is denoted by $\mathcal{C}^j[0,\ T_f]$ for any $j \in \mathcal{N}$. The Euclidean norm of any vector, $\mathbf{x} \in \mathcal{R}^n$ is represented by $|\mathbf{x}|$, and $|\mathbf{x}|^2 \triangleq \mathbf{x}^\intercal \mathbf{x}$. For any matrix $A \in \mathcal{R}^{n\times m}$, $|A|$ represents the induced matrix norm. For a square matrix $A \in \mathcal{R}^{n\times n}$, $A > 0$ indicates A is a positive definite matrix. $(\cdot)^\intercal$ represents the transpose of a vector or a matrix. I_n denotes the identity matrix of dimension n. For any vector $\mathbf{u}^*$, $\mathbf{u}^* > 0$ indicates that all its elements are positive. $(\cdot)_i$ represents any signal at the i^{th}

Melbourne School of Engineering, The University of Melbourne, Parkville VIC 3010 Australia, E-mail: {gsebastian, zeyul5}@student.unimelb.edu.au, {yingt, doetomo}@unimelb.edu.au

iteration. Unless otherwise mentioned, the notion i represents the iteration number.

For any signal in $\mathcal{L}^2[0,T_f]$[1], its $\mathcal{L}^2$ norm is defined as $\|\mathbf{x}\|_{\mathcal{L}^2} \triangleq \left(\int_0^{T_f} |\mathbf{x}(\tau)|^2 d\tau\right)^{\frac{1}{2}}$.

Let $u \in R$ and $u^* > 0$. The saturation function is defined as $\mathrm{sat}(u,u^*) \triangleq sign(u)\, min\{u^*, |u|\}$ for any $u \in \mathcal{R}$. For any $\mathbf{u} \in \mathcal{R}^m$ and a positive vector $\mathbf{u}^*$, the saturation function is defined as $\mathrm{sat}(\mathbf{u},\mathbf{u}^*) = \left[\mathrm{sat}(u^1, u^{1^*}), \cdots, \mathrm{sat}(u^m, u^{m^*})\right]^{\mathsf{T}}$.

The following lemmas will be used to facilitate the proof of Theorem 1 in this paper.

Lemma 1: [18, Property-3] For any given $\mathbf{u}_r$, $\mathbf{u}$ and $\mathbf{u}^* \in \mathcal{R}^m$ satisfying $\mathrm{sat}(\mathbf{u}_r,\mathbf{u}^*) = \mathbf{u}_r$ then the following inequality holds: $|\mathbf{u}_r - \mathrm{sat}(\mathbf{u},\mathbf{u}^*)|^2 \le |\mathbf{u}_r - \mathbf{u}|^2$. □

Lemma 2: [18, Property-4] For any $\mathbf{u}$, $\mathbf{u}^*$ and $\mathbf{w} \in \mathcal{R}^m$ satisfying $\mathbf{u}^* > 0$, if $\mathbf{v} = \mathrm{sat}(\mathbf{u},\mathbf{u}^*) + \mathbf{w}$, then the following inequality holds: $|\mathrm{sat}(\mathbf{v},\mathbf{u}^*) - \mathbf{v}| \le |\mathbf{w}|$. □

A. Problem Formulation

The equations of motion of a direct drive, fully actuated robotic manipulator with n rigid link can be represented as [19]

$$\begin{aligned} M(\boldsymbol{\theta})\ddot{\boldsymbol{\theta}} + C(\boldsymbol{\theta},\dot{\boldsymbol{\theta}})\dot{\boldsymbol{\theta}} + \mathbf{f}(\dot{\boldsymbol{\theta}}) + \mathbf{g}(\boldsymbol{\theta}) &= \mathbf{u} \\ \mathbf{u} &= \mathrm{sat}(\mathbf{v},\mathbf{u}^*) \\ \mathbf{y} &= \boldsymbol{\theta} \end{aligned} \tag{1}$$

where $\boldsymbol{\theta}, \dot{\boldsymbol{\theta}}$ and $\ddot{\boldsymbol{\theta}} \in \mathcal{R}^n$ are the vector of joint angles, velocities and accelerations respectively. The control input, $\mathbf{v} \in \mathcal{R}^n$ is the vector of applied input to the actuator. $M(\cdot) \in \mathcal{R}^{n\times n}$ is the inertia matrix, $C(\cdot,\cdot) \in \mathcal{R}^{n\times n}$ represents the total Coriolis and Centripetal terms, $\mathbf{f}(\cdot) \in \mathcal{R}^n$ is the friction component and $\mathbf{g}(\cdot) \in \mathcal{R}^n$ is the gravity force vector. The vector $\mathbf{u}^* > 0$ indicates the saturation limit of the actuator.

Remark 1: It is assumed that the precise knowledge of the model of the robotic manipulator is not known. Therefore, the proposed controller design can be treated as a model-free method. ∘

The following properties hold for the robotic manipulator systems (1) matrices/vectors [19]:

Property 1: For a given $\mathbf{u}^* > 0$, the trajectories of the system are bounded for any $t \in [0, T_f]$ □

Property 2: The inertia matrix $M(\cdot)$ in (1) is symmetric and positive definite. More precisely, there exist two positive constants μ_1 and μ_2, s.t $0 < \mu_1 I_n \le M(\cdot) \le \mu_2 I_n$. □

Property 3: The matrix $(\dot{M} - 2C)$ in (1) is a skew symmetric matrix. Hence for any $\mathbf{x} \in \mathcal{R}^n$, the following relation hold: $\mathbf{x}^{\mathsf{T}}(\dot{M} - 2C)\mathbf{x} = 0$. □

Property 4: For a given compact set $B_\Delta :\triangleq \{\mathbf{x} \in \mathcal{R}^n \mid |\mathbf{x}| \le \Delta\}$, there exist three positive constants C_b, F_b, and G_b such that: $\left|C(\boldsymbol{\theta},\dot{\boldsymbol{\theta}})\right| \le C_b \left|\dot{\boldsymbol{\theta}}\right|$, $\left|\mathbf{f}(\dot{\boldsymbol{\theta}})\right| \le F_b \left|\dot{\boldsymbol{\theta}}\right|$ and $|G(\boldsymbol{\theta})| \le G_b$, for any $\left[\begin{array}{cc} \boldsymbol{\theta}^{\mathsf{T}} & \dot{\boldsymbol{\theta}}^{\mathsf{T}} \end{array}\right]^{\mathsf{T}} \in B_\Delta$. □

[1]The space of $\mathcal{L}^2[0,T_f]$ contains all square-integrable functions over a finite interval $[0,T_f]$

Remark 2: Property 1 comes from passivity property of robotic manipulators [19]. Hence finite escape phenomenon will not happen. This indicates that the boundedness of the state trajectories for a finite time interval holds when the input is bounded. ∘

Remark 3: When comparing Property 2 and 3 which is defined globally, Property 4 holds locally as the constants in inequalities depend on the size of the compact set of the trajectories. If the system (1) is unstable, these constants will go to infinity. ∘

The equations of motion (1) can be represented by a multiple-input-multiple-output (MIMO) square[2] state-space form. At each iteration, this state-space form is:

$$\begin{aligned} \begin{pmatrix} \dot{\mathbf{x}}_{1,i} \\ \dot{\mathbf{x}}_{2,i} \end{pmatrix} &= \begin{pmatrix} \mathbf{x}_{2,i} \\ \mathbf{h}(\mathbf{x}_{1,i},\mathbf{x}_{2,i}) \end{pmatrix} + \begin{pmatrix} 0 \\ M^{-1}(\mathbf{x}_{1,i}) \end{pmatrix} \mathbf{u}_i \\ \mathbf{y}_i &= \mathbf{x}_{1,i}, \end{aligned} \tag{2}$$

where
$$\begin{aligned} \mathbf{h}(\mathbf{x}_{1,i},\mathbf{x}_{2,i}) \triangleq\; & -M^{-1}(\mathbf{x}_{1,i})C(\mathbf{x}_{1,i},\mathbf{x}_{2,i})\mathbf{x}_{2,i} \\ & -M^{-1}(\mathbf{x}_{1,i})\left(\mathbf{f}(\mathbf{x}_{2,i}) + \mathbf{g}(\mathbf{x}_{1,i})\right). \end{aligned}$$

Here, $\mathbf{x}_{1,i} = \boldsymbol{\theta}_i$ and $\mathbf{x}_{2,i} = \dot{\boldsymbol{\theta}}_i$ are the state and $\mathbf{y}_i$ is the output which is the joint position vector.

Remark 4: The robotic manipulator system is defined in joint space with joint positions as the system output. This system has the relative degree 2. Without any loss of generality, it is possible to extend the control design and analysis made in this paper even if the output is defined in task space instead of joint space using an appropriate Jacobian transformation. ∘.

The following assumptions are needed in this paper.

Assumption 1: For a given $\mathbf{y}_r = \mathbf{x}_{1,r} \in \mathcal{C}^1[0,\ T_f]$, there are reference state $\mathbf{x}_{2,r} \in \mathcal{C}^1[0,\ T_f]$ and reference input $\mathbf{u}_r \in \mathcal{C}[0,\ T_f]$ that satisfy the following dynamics

$$\begin{pmatrix} \dot{\mathbf{x}}_{1,r} \\ \dot{\mathbf{x}}_{2,r} \end{pmatrix} = \begin{pmatrix} \mathbf{x}_{2,r} \\ \mathbf{h}(\mathbf{x}_{1,r},\mathbf{x}_{2,r}) \end{pmatrix} + \begin{pmatrix} 0 \\ M^{-1}(\mathbf{x}_{1,r}) \end{pmatrix} \mathbf{u}_r \tag{3}$$

Moreover, there exists a known positive vector $\mathbf{u}^*$ such that $\mathrm{sat}(\mathbf{u}_r,\mathbf{u}^*) = \mathbf{u}_r$, $\forall t \in [0,\ T_f]$ is satisfied. □

Remark 5: Assumption 1 is presented for a general class of nonlinear systems. It implies the existence of ideal trajectories and ideal input signals that coming from the same model. It is not restrictive for many practical problems. For example, this assumption holds true for robotic manipulators. Moreover, this assumption also indicates that the ideal input signal is realizable within the limits of actuator constraints. This assumption plays an important role in the analysis if a class of general nonlinear systems is considered. ∘

Remark 6: This paper shows that the input signal will converge to the ideal input signal with the help of Assumption 1. The convergence of input can be naturally link to input saturation, making the convergence analysis feasible in the presence of input saturation. ∘

The output tracking error is defined as

$$\mathbf{e}_i(t) \triangleq \mathbf{y}_r(t) - \mathbf{y}_i(t) \tag{4}$$

[2] A square system has same the dimension for input and output vectors.

Assumption 2: The system (2) performs repetitive tracking with a finite time interval $[0, T_f]$. Moreover, the identical initial condition $\mathbf{e}_i(0) = \dot{\mathbf{e}}_i(0) = 0$ is satisfied in all iterations. □

Remark 7: The Assumption 2 is a standard assumption in the ILC design. It is possible to relax this assumption at the expense of sacrificing the perfect tracking performance. For more details, refer [20] and references therein. ∘

The control objective is to design a sequence of control input signal to achieve a perfect tracking performance in the presence of actuator saturation. More precisely, the objective is to find a sequence of control input $\{\mathbf{u}_i\}_{i\in\mathcal{N}_{\geq 0}}$ such that the tracking error converges point-wisely, i.e. $\lim_{i\to\infty} |\mathbf{e}_i(t)| = 0$.

III. Proposed control structure with convergence analysis

The proposed structure is shown in Fig.1. It consists of a

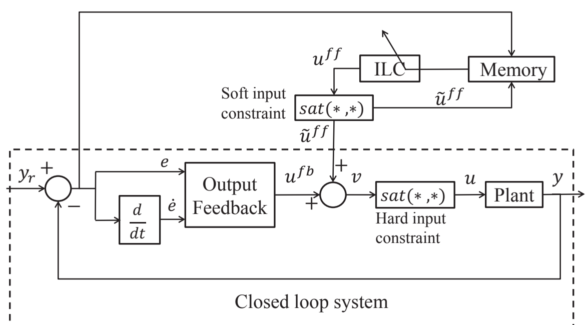

Fig. 1. Block diagram of proposed control architecture

standard PD-type feedback control $\mathbf{u}^{fb}$ with a modified PD-type feed-forward ILC $\mathbf{u}^{ff}$. The control input applied to the plant takes the following form

$$\mathbf{v}_i(t) = \tilde{\mathbf{u}}_i^{ff}(t) + \mathbf{u}_i^{fb}(t),\ \forall t \in [0,\ T_f],\ i = 1, 2, \cdots,. \quad (5)$$

where $\tilde{\mathbf{u}}_i^{ff}(t) \triangleq \mathrm{sat}(\mathbf{u}_i^{ff}(t),\ \mathbf{u}^*)$, the feed-forward control input $\mathbf{u}_i^{ff}(t)$ is given by

$$\mathbf{u}_{i+1}^{ff}(t) = \tilde{\mathbf{u}}_i^{ff}(t) + \Gamma_p \mathbf{e}_i(t) + \Gamma_d \dot{\mathbf{e}}_i(t),\ \mathbf{u}_1^{ff}(t) = 0, \quad (6)$$

where Γ_p and $\Gamma_d \in \mathcal{R}^{n\times n}$ are diagonal matrices to be designed. Moreover, the feedback control $\mathbf{u}_i^{fb}(t)$ takes the following form:

$$\mathbf{u}_i^{fb}(t) = K_p \mathbf{e}_i(t) + K_d \dot{\mathbf{e}}_i(t). \quad (7)$$

where $K_p,\ K_d \in \mathcal{R}^{n\times n}$ are symmetric positive definite gain matrices for the feedback control.

Remark 8: The PD-type ILC law (6) is different from the one in [14] as the input saturation is considered. A saturated feed-forward ILC control input of the previous iteration, $\tilde{\mathbf{u}}_i^{ff}(t)$ is used in the update law, instead of $\mathbf{u}_i^{ff}(t)$. Furthermore, a soft input saturation is applied in the control structure to further ensure that the input constraint will be satisfied. With the hard input constraints (see Fig. 1), three saturation functions working together to ensure the boundedness and the convergence of the tracking error [21]. ∘

Remark 9: As the matrix $M(\cdot)$ is symmetric and positive definite and Γ_d is a positive diagonal matrix, the matrix $\Gamma_d M(\cdot)$ is always symmetric and positive definite. This property will be used in the proof of the main result. More precisely, there a positive constant γ such that the following condition holds:

$$0 < \gamma I_n \leq \Gamma_d M(\mathbf{x}_{1,i})$$

for all $\mathbf{x}_{1,i} \in \mathcal{R}^n$.

Remark 10: Without any loss of generality, a PD-type feedback is employed as it is widely used in the stabilization of robot manipulators. The role of such a feedback is to ensure uniform boundedness of trajectories in the presence of actuator saturation. When the trajectories are uniformly bounded, the local Lipschitz continuity can be treated as the global Lipschitz continuity . ∘

Next, the main result of this paper is presented in Theorem 1.

Theorem 1: Assume that the system (2) satisfies Assumptions 1 and 2. With the control laws (5), (6) and (7), the closed loop system can ensure that

1) The input signal $\mathbf{u}_i^{ff}$ converges to the desired control input $\mathbf{u}_r$ in $\mathcal{L}^2$ norm sense.
2) The tracking error converges to zero uniformly.

□

The proof of the theorem is given in Appendix .

Remark 11: In the proof of the theorem, a fictitious error, $\boldsymbol{\xi} \triangleq \dot{\mathbf{e}} + \Gamma_d^{-1}\Gamma_p \mathbf{e}$ is introduced to simplify the analysis. Then the convergence of $\boldsymbol{\xi}$ is achieved. The convergence of tracking error can still be guaranteed even if $\Gamma_p = 0$. This means that the ILC law includes only the derivative of previous iteration tracking error. ∘

IV. Simulation and Experimental Results

The effectiveness of the proposed controller is demonstrated using a simulation and an implementation in a robotic manipulator, EMU [22] which has three degrees of freedom as shown in Fig. 2. For the ease of presentation, only the last two degrees of freedom, θ_2 and θ_3, are used for illustration. The output reference trajectories which are used for the simulation and experiment are shown in Fig. 3. The following parameters are selected for the control law (5), $K_p = 3I_n$,$K_d = 0.1I_n$, $\Gamma_p = 0.4I_n$ and $\Gamma_d = 0.6I_n$ in simulation as well as in experimental validation. Without any loss of generality, a nominal gravity compensation is applied in control input to ensure the satisfaction of Assumption 2 in experiments. Similar condition is also imposed in simulations. A saturation limit, $\mathbf{u}^* = [1.5,\ 1.5]$ is chosen. The data is recorded with a sampling time of $0.001s$ in simulation and in experiments.

A. Simulation Results

The nominal model of the robot, EMU from [23] is used for simulations. Due to space constraints, the model details are omitted in this paper. The simulations are performed for

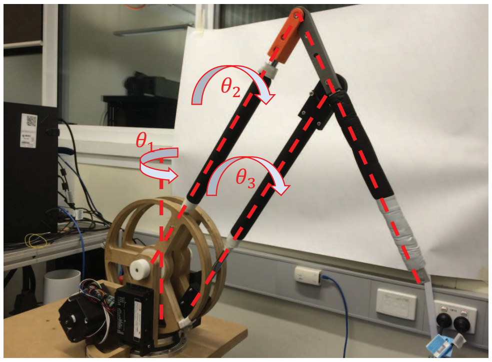

Fig. 2. Robotic manipulator with three actuated degrees of freedom

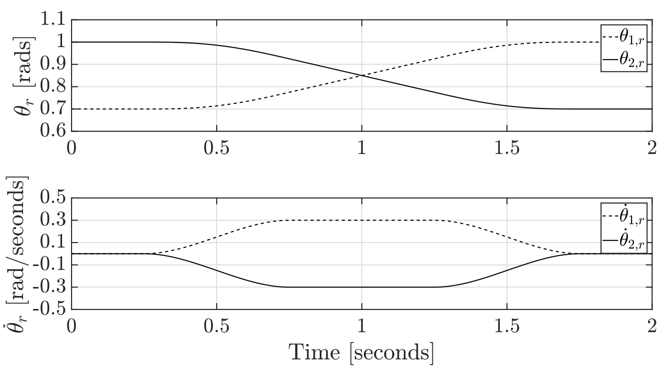

Fig. 3. The output references, $\boldsymbol{\theta} = \mathbf{x}_{r,1}$ and $\dot{\boldsymbol{\theta}} = \mathbf{x}_{r,2}$ used in experiments and simulations.

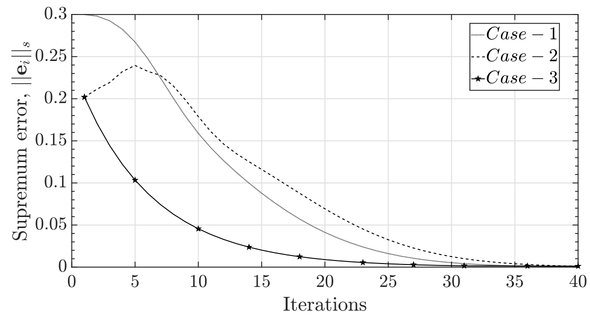

Fig. 4. Simulation results: Case-1 and Case-2 use double derivative of tracking error as proposed in [2], [12], Case-3 use PD type ILC with saturation constraints.

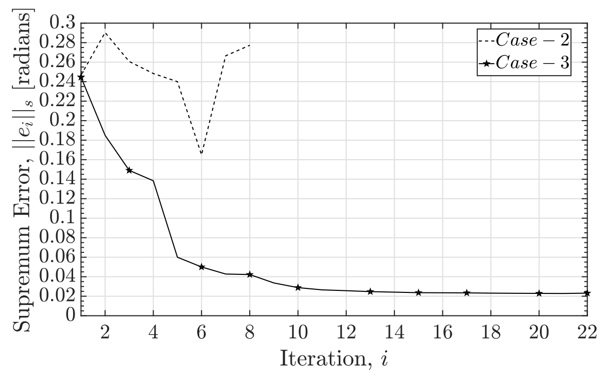

Fig. 5. Experimental Results: The variation of supremum norm of tracking error.

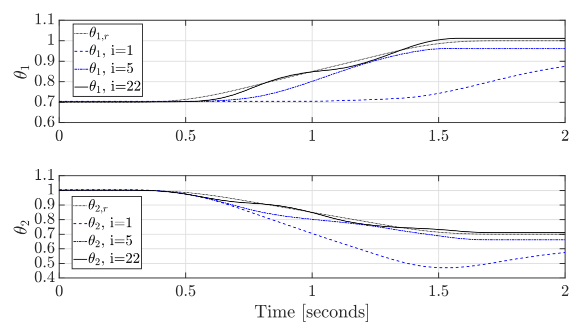

Fig. 6. Experimental Results: The output trajectories, θ_2 and θ_3 for $i = 1, 5, 22$ for Case -3 (Proposed ILC scheme).

the following three cases. For Case-1, the DD-type ILC is used for tracking without any feedback control. For Case 2, a PD type feedback is used along with Case-1 to indicate the difference in the transient performance in learning. Lastly, for Case-3, the tracking performance using the proposed ILC scheme in the presence of input saturation is presented. For Case-1, the update gain: $\begin{bmatrix} 0.394 & -0.124 \\ -0.124 & 0.342 \end{bmatrix}$ is used which satisfies the required convergence condition as given in [14]. The simulation is performed for 40 iterations. The variation of supremum norm[3] of tracking error is shown in Fig. 4.

As expected, the existence of the feedback has improved the transient performance in Case-2 and Case-3 when compared with Case-1. The proposed algorithm have a better transient performance than Case-1 and Case-2, though the improvement is not significant. It will show next that implementing Case-2 faces much difficulty in experiments due to unreliable second derivative information in the update law.

B. Experimental Results

The experiment is performed using the ILC which needs the double derivative of output tracking error (Case-2) as well as the proposed ILC scheme (Case-3) in the presence hard input constraints (Case-3).

The derivative of the tracking error is calculated using the backward difference method. A Butterworth filter of order 4, with cut-off frequency of $60Hz$ is used to eliminate the noises in $\dot{\mathbf{e}}$ and $\mathbf{u}^{ff}$ for a PD type ILC. For DD-type ILC, a second Butterworth filter of order 4 with a lower cut-off frequency of $10Hz$ is used to numerically differentiate the derivative of the tracking error.

The experiments have been carefully designed to satisfy the identical initial condition as Assumptions 2 is critical in

[3]If a function is in $\mathcal{L}_\infty[0,T]$, which is the space consisting of all essentially bounded signals, $\|\mathbf{x}\|_s = \max_{t\in[0,T_f]} |\mathbf{x}(t)|$.

achieving the convergence. In order to achieve Assumption 2, a PID controller is used to initialize the tracking in the same position with an error norm less than 0.005 radians. The experiment is performed for 8 iterations for DD-ILC and 22 iterations for proposed ILC scheme. The variation of supremum norm of tracking error for both cases are shown in Fig. 5. The supremum norm of the error converges when the iteration progresses with PD type ILC whereas due to unreliable values of second derivative signal, the convergence is affected for a DD-ILC. Hence the trials are stopped after 8 iterations. The output trajectories for Case 3 at iterations $i = 1, 5, 22$ along with the reference trajectory is shown in Fig. 6. It can be seen that the trajectories are converged to reference trajectory with a maximum error of nearly 0.02 radians for PD type ILC. It is found that the implementation using PD type ILC is more robust to measurement noises in experiments.

V. Conclusion

This paper presented a feedback-based PD-type ILC algorithm for robotic manipulators with position output (or the system with the relative degree two) in the presence of hard input constraints. By using composite energy function, the main result shows that the tracking error converges uniformly and the control input is always bounded in $\mathcal{L}^2$ norm. Simulations and experimental results illustrate the effectiveness of the proposed method.

Appendix
Proof of Theorem 1

Proof: For the convenience of the proof, the following variables are defined. A fictitious reference signal is introduced, which is defined as

$$\overline{\mathbf{u}}_r \triangleq M(\mathbf{x}_1)M^{-1}(\mathbf{x}_{1,r})\mathbf{u}_r. \tag{8}$$

Because of Property 2, $\overline{\mathbf{u}}_r$ is continuous and bounded. When the output trajectory $\mathbf{y}$ approaches the reference trajectory $\mathbf{y}_r$, then the fictitious reference input, $\overline{\mathbf{u}}_r$ approaches the actual reference input $\mathbf{u}_r$.

A new fictitious velocity error is defined as:

$$\boldsymbol{\xi} \triangleq \dot{\mathbf{e}} + \Gamma_d^{-1}\Gamma_p\mathbf{e} \tag{9}$$

Due to Assumption 2, if $\boldsymbol{\xi} \to 0$, then $\mathbf{e} \to 0$. The feedback control (7) can be represented in terms of fictitious velocity error as

$$\mathbf{u}^{fb} = K_d\boldsymbol{\xi} + \hat{K}_p\mathbf{e} \tag{10}$$

where $\hat{K}_p \triangleq K_p - K_d\Gamma_d^{-1}\Gamma_p$. Finally for the simplification of notations, let $M \triangleq M(\mathbf{x}_1)$, $C \triangleq C(\mathbf{x}_1, \mathbf{x}_2)$, $\delta\mathbf{h} \triangleq \mathbf{h}(\mathbf{x}_{1,r}, \mathbf{x}_{2,r}) - \mathbf{h}(\mathbf{x}_1, \mathbf{x}_2)$, $\delta\mathbf{u} \triangleq \overline{\mathbf{u}}_r - \mathbf{u}$, $\delta\mathbf{u}^{ff} \triangleq \overline{\mathbf{u}}_r - \mathbf{u}^{ff}$ and $\delta\widetilde{\mathbf{u}}^{ff} \triangleq \overline{\mathbf{u}}_r - \widetilde{\mathbf{u}}^{ff}$.

Differentiating (9) with respect to time followed by multiplying with inertia matrix M yields:

$$\begin{aligned} M\dot{\boldsymbol{\xi}} =& M\ddot{\mathbf{e}} + M\Gamma_d^{-1}\Gamma_p\dot{\mathbf{e}} = M\delta\mathbf{h} + \delta\mathbf{u} + M\Gamma_d^{-1}\Gamma_p\dot{\mathbf{e}} \\ =& \delta\mathbf{u} - C\boldsymbol{\xi} + \boldsymbol{\zeta} \\ =& \delta\widetilde{\mathbf{u}}^{ff} - \mathbf{u}^{fb} - (\mathrm{sat}(\mathbf{v}, \mathbf{u}^*) - \mathbf{v}) - C\boldsymbol{\xi} + \boldsymbol{\zeta} \end{aligned} \tag{11}$$

where $\boldsymbol{\zeta} \triangleq M\delta\mathbf{h} + C\boldsymbol{\xi} + M\Gamma_d^{-1}\Gamma_p\dot{\mathbf{e}}$.

Consider the energy function $J_i(t)$:

$$J_i(t) = \int_0^t e^{-\lambda\tau}\delta\mathbf{u}_i^{ff\intercal}(\tau)\delta\mathbf{u}_i^{ff}(\tau)d\tau, \tag{12}$$

where λ is any positive constant. This energy function is a time-weighted $\mathcal{L}^2$ norm of $\delta\mathbf{u}_i^{ff}$ which is equivalent to the one used in [14] which captures the learning in the iteration domain.

The proof is divided into mainly two parts. The first part shows that the proposed energy function is non-increasing in the iteration domain, followed by the second part where the convergence of output tracking error is established.

A non-increasing property of the energy function (12) in the iteration domain is established. This means that if J_i is bounded, J_{i+1} is also bounded.

A. Non-increasing Energy Function

The difference of energy function between two iterations is given by

$$\Delta J_{i+1} = J_{i+1} - J_i = \int_0^t e^{-\lambda\tau}\left(\left|\delta\mathbf{u}_{i+1}^{ff}\right|^2 - \left|\delta\mathbf{u}_i^{ff}\right|^2\right)d\tau \tag{13}$$

Due to Lemma 1, the following relation holds:

$$\left|\delta\mathbf{u}_{i+1}^{ff}\right|^2 - \left|\delta\mathbf{u}_i^{ff}\right|^2 \le \left|\delta\mathbf{u}_{i+1}^{ff}\right|^2 - \left|\delta\widetilde{\mathbf{u}}_i^{ff}\right|^2 \tag{14}$$

In addition, the ILC law (6) can be written in terms $\boldsymbol{\xi}$ as follows:

$$\delta\mathbf{u}_{i+1}^{ff} = \delta\widetilde{\mathbf{u}}_i^{ff} - \Gamma_d\boldsymbol{\xi}_i. \tag{15}$$

Therefore substituting equation (14) followed by (15) back into (13) yields:

$$\begin{aligned} \Delta J_{i+1} \le& \int_0^t e^{-\lambda\tau}\left(\left|\delta\mathbf{u}_{i+1}^{ff}\right|^2 - \left|\delta\widetilde{\mathbf{u}}_i^{ff}\right|^2\right)d\tau \\ \le& -2\int_0^t e^{-\lambda\tau}(\Gamma_d\boldsymbol{\xi}_i)^\intercal\delta\widetilde{\mathbf{u}}_i^{ff}d\tau + \int_0^t e^{-\lambda\tau}\left|\Gamma_d\boldsymbol{\xi}_i\right|^2 d\tau. \end{aligned} \tag{16}$$

The equation (16) consists of two control signals $\boldsymbol{\xi}_i$ and $\delta\widetilde{\mathbf{u}}_i^{ff}$ of i^{th} iteration. Using the error dynamics from (11), equation (16) can be written in term of $\boldsymbol{\xi}_i$ and $\dot{\boldsymbol{\xi}}_i$. Therefore substituting $\delta\widetilde{\mathbf{u}}_i^{ff}$ from (11) into (16) yields

$$\begin{aligned} \Delta J_{i+1} \le& -2\int_0^t e^{-\lambda\tau}(\Gamma_d\boldsymbol{\xi}_i)^\intercal M_i\dot{\boldsymbol{\xi}}_i d\tau \\ &-2\int_0^t e^{-\lambda\tau}(\Gamma_d\boldsymbol{\xi}_i)^\intercal\mathbf{u}_i^{fb}d\tau \\ &-2\int_0^t e^{-\lambda\tau}(\Gamma_d\boldsymbol{\xi}_i)^\intercal\left(\mathrm{sat}(\mathbf{v}_i, \mathbf{u}^*) - \mathbf{v}_i\right)d\tau \\ &-2\int_0^t e^{-\lambda\tau}(\Gamma_d\boldsymbol{\xi}_i)^\intercal C_i\boldsymbol{\xi}_i d\tau \\ &+\int_0^t e^{-\lambda\tau}(\Gamma_d\boldsymbol{\xi}_i)^\intercal\left(2\boldsymbol{\zeta}_i + \Gamma_d\boldsymbol{\xi}_i\right)d\tau. \end{aligned} \tag{17}$$

To eliminate the derivative of $\boldsymbol{\xi}$ from (17), the following equality can be used for the first term in (17),

$$
\begin{aligned}
&-2e^{-\lambda t}(\Gamma_d \boldsymbol{\xi}_i)^\intercal M\dot{\boldsymbol{\xi}}_i \\
&= -\frac{d}{dt}\left(e^{-\lambda t}(\Gamma_d \boldsymbol{\xi}_i)^\intercal M_i \boldsymbol{\xi}_i\right) + e^{-\lambda t}(\Gamma_d \boldsymbol{\xi}_i)^\intercal \dot{M}_i \boldsymbol{\xi}_i \\
&\quad - \lambda e^{-\lambda t}(\Gamma_d \boldsymbol{\xi}_i)^\intercal M_i \boldsymbol{\xi}_i. \qquad (18)
\end{aligned}
$$

Due to Lemma 2, $|\mathrm{sat}(\mathbf{v}_i, \mathbf{u}^*) - \mathbf{v}_i| \le \left|\mathbf{u}_i^{fb}\right|$. Using Property 3, identical initial condition (Assumption 2) and the equation (18), the difference in energy function, (17) can be re-written as

$$
\begin{aligned}
\Delta J_{i+1} \le &- e^{-\lambda t}(\Gamma_d \boldsymbol{\xi}_i)^\intercal M_i \boldsymbol{\xi}_i \\
&- \lambda \int_0^t e^{-\lambda \tau}(\Gamma_d \boldsymbol{\xi}_i)^\intercal M_i \boldsymbol{\xi}_i d\tau \\
&+ \int_0^t e^{-\lambda \tau}(\Gamma_d \boldsymbol{\xi}_i)^\intercal \left(2\boldsymbol{\zeta}_i + \Gamma_d \boldsymbol{\xi}_i\right) d\tau \\
&+ 4\int_0^t e^{-\lambda \tau} \left|\Gamma_d \boldsymbol{\xi}_i\right| \left|\mathbf{u}_i^{fb}\right| d\tau. \qquad (19)
\end{aligned}
$$

It is possible to show that there exists two positive constants c_1 and c_2 such that the following inequality holds:

$$
|\boldsymbol{\zeta}| \le c_1 |\boldsymbol{\xi}| + c_2 |\boldsymbol{\xi}|^2. \qquad (20)
$$

For a given compact set B_Δ, there exists a positive constant $c_3 = c_3(\Delta)$ such that $\left|\mathbf{u}_i^{fb}\right| \le c_3 |\boldsymbol{\xi}_i|$. Because of Property 2, M_i is symmetric and positive definite. If Γ_d is chose in such a way that $\Gamma_d M_i$ is symmetric and positive definite, then there exists a $\gamma > 0$ such that $0 < \gamma I_n < \Gamma_d M(\mathbf{x}_{1,i})$ for all $\mathbf{x}_i \in B_\Delta$:

$$
\begin{aligned}
\Delta J_{i+1} \le &- \gamma e^{-\lambda t} |\boldsymbol{\xi}_i|^2 - \lambda\gamma \int_0^t e^{-\lambda \tau} |\boldsymbol{\xi}_i|^2 d\tau \\
&+ \int_0^t e^{-\lambda \tau} R(|\boldsymbol{\xi}_i|) d\tau \qquad (21)
\end{aligned}
$$

where $R(|\boldsymbol{\xi}_i|) = r_0 |\boldsymbol{\xi}_i|^2 + r_1 |\boldsymbol{\xi}_i|^3$ is a polynomial function in $|\boldsymbol{\xi}|$, $r_0 = |\Gamma_d|\,(2c_1 + |\Gamma_d| + 4|\Gamma_d|\, c_3)$, $r_1 = 2|\Gamma_d|\, c_2$. For any compact set B_Δ, there exists a constant $c_4 = c_4(\Delta)$ such that

$$
R(|\boldsymbol{\xi}_i|) \le c_4 |\boldsymbol{\xi}_i|^2
$$

For any $c_5 > 0$, by selecting $\lambda > c_4 + c_5$, it follows that

$$
\Delta J_{i+1} \le \quad -\gamma e^{-\lambda t} |\boldsymbol{\xi}_i|^2 - c_5 \gamma \int_0^t e^{-\lambda \tau} |\boldsymbol{\xi}_i|^2 d\tau \le 0
$$

B. Convergence Property

Barbalet Lemma can be applied to ensure the uniform convergence property. As J_1 is bounded, $J_i(t)$ is non-increasing in the iteration axis, the pointwise convergence of input signal in terms of $\mathcal{L}^2$ norm can be obtained. This suggests that the tracking error converges point-wisely. In addition, the uniform boundedness of (11) ensures the uniform continuity of $\boldsymbol{\xi}_i$ in the interval $[0, T_f]$. This leads to the uniform convergence of the tracking error.

This completes the proof. ■

REFERENCES

[1] M. Uchiyama, "Formation of high-speed motion pattern of a mechanical arm by trial," *Transactions of the Society of Instrument and Control Engineers*, vol. 14, no. 6, pp. 706–712, 1978.

[2] S. Arimoto, S. Kawamura, and F. Miyazaki, "Bettering operation of robots by learning," *Journal of Robotic systems*, vol. 1, no. 2, pp. 123–140, 1984.

[3] M. Mezghani, G. Roux, M. Cabassud, M. V. Le Lann, B. Dahhou, and G. Casamatta, "Application of iterative learning control to an exothermic semibatch chemical reactor," *IEEE Transactions on Control Systems Technology*, vol. 10, no. 6, pp. 822–834, 2002.

[4] E. Rogers and O. R. Tutty, "Iterative learning control with applications in energy generation, lasers and health care," *Proceedings of the Royal Society of London A: Mathematical, Physical and Engineering Sciences*, vol. 472, no. 2193, 2016.

[5] R. W. Longman, "Iterative learning control and repetitive control for engineering practice," *International journal of control*, vol. 73, no. 10, pp. 930–954, 2000.

[6] Z. Hou, J.-X. Xu, and J. Yan, "An iterative learning approach for density control of freeway traffic flow via ramp metering," *Transportation Research Part C: Emerging Technologies*, vol. 16, no. 1, pp. 71–97, 2008.

[7] D. A. Bristow, M. Tharayil, and A. G. Alleyne, "A survey of iterative learning control," *IEEE Control Systems*, vol. 26, no. 3, pp. 96–114, 2006.

[8] H.-S. Ahn, Y. Chen, and K. L. Moore, "Iterative learning control: brief survey and categorization," *IEEE Transactions on Systems Man and Cybernetics Part C Applications and Reviews*, vol. 37, no. 6, p. 1099, 2007.

[9] P. Bondi, G. Casalino, and L. Gambardella, "On the iterative learning control theory for robotic manipulators," *IEEE Journal on Robotics and Automation*, vol. 4, no. 1, pp. 14–22, 1988.

[10] M. Norrlof, "An adaptive iterative learning control algorithm with experiments on an industrial robot," *IEEE Transactions on robotics and automation*, vol. 18, no. 2, pp. 245–251, 2002.

[11] A. Tayebi and S. Islam, "Adaptive iterative learning control for robot manipulators: Experimental results," *Control Engineering Practice*, vol. 14, no. 7, pp. 843–851, 2006.

[12] H.-S. Ahn, C.-H. Choi, and K.-b. Kim, "Iterative learning control for a class of nonlinear systems," *Automatica*, vol. 29, no. 6, pp. 1575–1578, 1993.

[13] S. Kawamura, F. Miyazaki, and S. Arimoto, "Realization of robot motion based on a learning method," *IEEE Transactions on Systems, Man, and Cybernetics*, vol. 18, no. 1, pp. 126–134, 1988.

[14] S. Arimoto, "Learning control theory for robotic motion," *International Journal of Adaptive Control and Signal Processing*, vol. 4, no. 6, pp. 543–564, 1990.

[15] Y. Tan, S. P. Yang, and J. X. Xu, "On P-type iterative learning control for nonlinear systems without global Lipschitz continuity condition," in *American Control Conference (ACC), 2015*. IEEE, 2015, pp. 3552–3557.

[16] G. Sebastian, Y. Tan, and D. Oetomo, "Convergence analysis of feedback-based iterative learning control with input saturation," *Automatica*, vol. 101, pp. 44–52, 2019.

[17] G. Sebastian, Y. Tan, D. Oetomo, and I. Mareels, "On feedback-based iterative learning control for nonlinear systems without global lipschitz continuity," in *2018 Annual American Control Conference (ACC)*. IEEE, 2018, pp. 5612–5617.

[18] J.-X. Xu, Y. Tan, and T.-H. Lee, "Iterative learning control design based on composite energy function with input saturation," *Automatica*, vol. 40, no. 8, pp. 1371–1377, aug 2004.

[19] F. L. Lewis, D. M. Dawson, and C. T. Abdallah, *Robot Manipulator Control: Theory and Practice*, 2nd ed. New York:Marcel Dekker, 2004.

[20] J.-X. Xu and R. Yan, "On initial conditions in iterative learning control," *IEEE Transactions on Automatic Control*, vol. 50, no. 9, pp. 1349–1354, 2005.

[21] G. Sebastian, Y. Tan, D. Oetomo, and I. Mareels, "On input and output constraints in iterative learning control design for robotic manipulators," *Unmanned Systems*, vol. 06, no. 03, pp. 197–208, 2018.

[22] J. Fong, V. Crocher, Y. Tan, D. Oetomo, and I. Mareels, "EMU: A transparent 3d robotic manipulandum for upper-limb rehabilitation," in *2017 International Conference on Rehabilitation Robotics (ICORR)*. IEEE, 2017, pp. 771–776.

[23] G. Sebastian, Y. Tan, D. Oetomo, and I. Mareels, "Feedback-based iterative learning design and synthesis with output constraints for robotic manipulators," *IEEE Control Systems Letters*, vol. 2, no. 3, pp. 513–518, July 2018.